Simulating Post Punching Behaviour of RC Slab-Column Connections Using a Micro Model

Huizhong Xue[1, a *], Hong Guan[1, b], Xinzheng Lu[2, c], and Yi Li[3, d]

[1]Griffith School of Engineering, Griffith University, Gold Coast Campus, QLD 4222, Australia

[2]Tsinghua University, Beijing, 100084, China

[3]Beijing University of Technology, Beijing 100124, China

[a]huizhong.xue@griffithuni.edu.au, [b]h.guan@griffith.edu.au, [c]luxz@tsinghua.edu.cn, [d]yili@bjut.edu.cn

Keywords: Micro numerical model; Post punching behaviour; Slab-column connection; Progressive collapse.

Abstract. Punching shear is a common failure mode occurring at the slab-column connection region of a reinforced concrete (RC) flat plate. Progressive collapse of RC flat plates poses a significant scientific question on the post punching behaviour of such a structural system. The challenge lies in the complex interactions amongst various internal actions including large unbalanced moments and shear forces. Existing numerical models are unable to differentiate the influence of each individual action within the connection region after punching occurs. Therefore, a new numerical model is required to model these actions individually as well as to evaluate their interrelationships. This paper thus aims to propose a numerical method to investigate the structural response of RC slab-column connections by using a micro model, based on a representative post punching failure experiment. In the micro model, concrete is simulated using solid elements whilst the reinforcement is modelled with truss elements. In this micro model, the constitutive laws and failure criteria of materials play a crucial role in describing the model's structural behaviour. A typical structural response is discussed and a calibration method is established. Ultimately this study is expected to facilitate the development of an effective, yet simplified numerical model for future progressive collapse simulation of slab-column connections.

Introduction

Punching shear is a common failure mode occurring at the slab-column connection region of a RC flat plate. When it comes to a column loss scenario, this structural failure may likely take place in the slab at the column removal position and adjacent column positions due to load redistribution. Gross deformation and subsequent failure of the slabs would likely lead to progressive collapse of the entire structural system. It is expected that an RC flat plate itself has a secondary load-bearing mechanism to resist progressive collapse after punching occurs. This requires the development of a set of effective design and construction measurements, based on a sound knowledge of the post punching behaviour of RC slab-column connections. This paper thus aims to propose a numerical method for investigating the structural response of RC slab-column connections by using a micro model. The modelling process is illustrated with particular emphasis on the material properties as they are the key controlling factors influencing the structural response of the model. Finally, a calibration method is described based on the analysis of a typical response of the model.

Overview of Slab-Column Joint Test

To investigate post punching behaviour, a series of RC slab-column joint specimens have been tested to failure at Tsinghua University, China. The loading process of one representative specimen (Fig. 1(a)) is simulated herein. The slab was monolithically casted with boundary beams which were designed as doubly reinforced. The specimen was fully fixed at four corners and loaded by a hydraulic jack at the top of the column stub using the displacement-controlled method. The materials

used were C30 concrete and 400MPa reinforcement. The top reinforcement ratios in the slab were 4.78% and 1.95% for the column strip and middle strip, respectively. The bottom reinforcement ratio of 1.95% was adopted for the entire slab. Although the loading process is pseudo-static, the actual punching shear failure exhibits brittle behaviour and transpires within a second. Therefore a general purpose finite element program LS-DYNA, which is capable of analysing highly nonlinear and transient dynamic behaviour using explicit time integration, is employed [1].

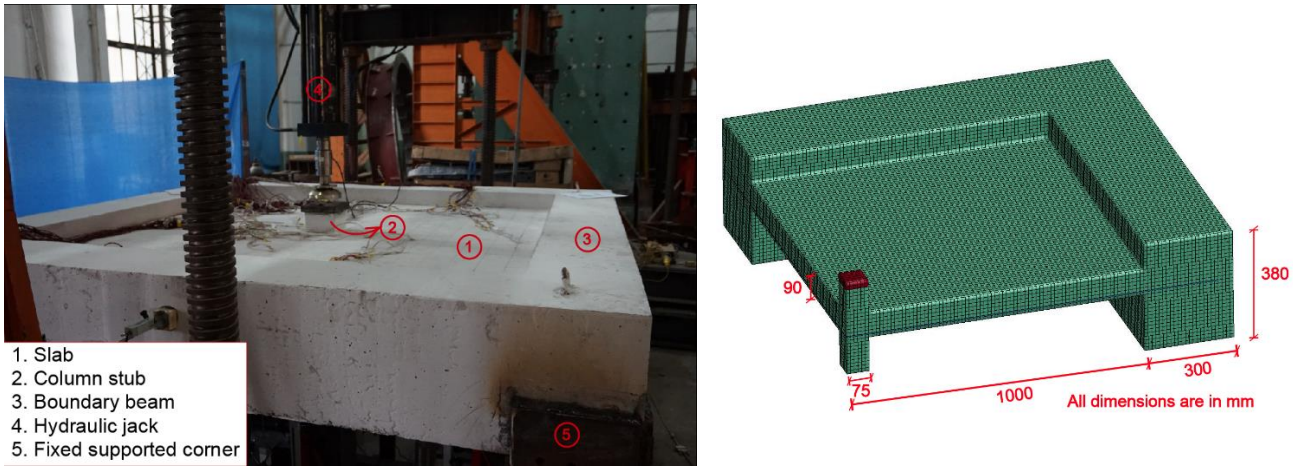

(a) (b)

Fig. 1 Slab-column joint (a) Test specimen (b) Micro numerical model (quarter model)

Micro Numerical Model

General. The discrete modelling strategy [2], which describes concrete and reinforcing bars separately using different elements, is adopted to create the RC slab-column joint model (Fig. 1(b)). Given the symmetrical property of the specimen, a 1/4 joint is modelled, which considerably increases the computational efficiency. The concrete is modelled using 8-node solid elements whilst the reinforcement is modelled with two-node truss elements. To ensure perfect bond between concrete and reinforcement elements and take the concrete cover into account, the smallest mesh size is set to 12.5mm. It should be noted that, in LS-DYNA, the time step may vary to achieve a better computational efficiency. Nevertheless, it is determined herein by the smallest mesh size to ensure numerical stability of the solution process.

Reinforcement. Reinforcement is modelled as elastoplastic material with isotropic hardening (*MAT_003 in LS-DYNA) as the specimen is monotonically loaded. The isotropic hardening effect is obtained as the subsequent yield surface radii increase as a function of the plastic strain given in Eq.1 [1].

$$\sigma_y = \sigma_0 + \beta E_p \varepsilon_{eff}^p \tag{1}$$

where, σ_0 is the initial yield strength, β is the hardening parameter taken as 1 for isotropic hardening, E_p is the plastic hardening modulus, and ε_{eff}^p is the effective plastic strain.

In addition, a dynamic increase factor $\mathrm{DIF} = \left(\dot{\varepsilon}/10^{-4}\right)^{\alpha}$ is applied to the subsequent yield surface to consider the strain rate ($\dot{\varepsilon}$) effect [1, 3]. The parameter α is a constant calculated by Eq.2, where f_y is the reinforcement yield strength in MPa.

$$\alpha = 0.074 - 0.040 f_y / 414 \tag{2}$$

Concrete. A calibrated Ben-Gurion University (BGU) model based on a plastic damage Karagozian & Case (K&C) model (*MAT_072R3 in LS-DYNA) is utilised to describe the hardening and softening effects of the concrete [4-6]. In the analysis, after solving the dynamic equations in each step, the displacements obtained are used to calculate the strains through geometric equations. On the other hand, the total stress tensor is partitioned into volumetric and deviatoric components. Further,

hydraulic pressure ($p = I_1/3$, I_1 is the first invariant of stress tensor) is calculated through an equation of state (EOS) including the volumetric strain ε_v which is determined by adding strains in three orthogonal directions. Three fixed failure surfaces are defined as functions of pressure p to limit the hardening and softening, or damage, after concrete enters the plastic deformation stage (Eq.3) [4, 6]. $\Delta\sigma_m$, $\Delta\sigma_r$ and $\Delta\sigma_y$ are the failure surfaces with respect to the deviatoric stresses ($\sqrt{3J_2}$, J_2 is the second invariant of the deviatoric stress tensor) and eight α parameters are determined via material testing. Eight empirical formulas for calculating these parameters were given in [6], which are reproduced in Eq.4. The α values for the test specimen are calculated and listed in Table 1.

$$\left.\begin{aligned} \Delta\sigma_m &= \alpha_0 + \frac{p}{\alpha_1 + \alpha_2 p} && \text{(maximum failure surface)} \\ \Delta\sigma_r &= \frac{p}{\alpha_{1f} + \alpha_{2f} p} && \text{(residual failure surface)} \\ \Delta\sigma_y &= \alpha_{0y} + \frac{p}{\alpha_{1y} + \alpha_{2y} p} && \text{(yield failure surface)} \end{aligned}\right\} \quad (3)$$

$$\left.\begin{aligned} &\alpha_0 = 2.442 f_c'^{-0.4369} && \alpha_1 = 1.084 f_c'^{-0.2436} && \alpha_2 = 0.03276 f_c'^{-0.6416} \\ &\alpha_{1f} = 0.4773 && \alpha_{2f} = 0.11/f_c' \\ &\alpha_{0y} = 2.525\ln(f_c' - 15.18) && \alpha_{1y} = 1.846 f_c'^{-0.2706} && \alpha_{2y} = 0.03181 f_c'^{-0.5355} \end{aligned}\right\} \quad (4)$$

Table 1 Values of α for the test specimen

α_0	α_1	α_2	α_{1f}	α_{2f}	α_{0y}	α_{1y}	α_{2y}
9.9657	0.4906	4.1536×10^{-3}	0.4773	4.4×10^{-3}	5.7682	0.7726	5.675×10^{-3}

Consequently, an expandable failure surface is able to be defined as Eq.5 and Eq.6 in which η is a function in terms of the modified effective plastic strain λ and takes the range of 0~1. Therefore, Eq. 5 and Eq.6 control, respectively, concrete hardening after the yield failure surface is reached and softening after the maximum failure surface is reached. In LS-DYNA, this $\eta - \lambda$ function is input as 13 pairs under the keyword *MAT_CONCRETE_DAMAGE_REL3. The suggested input for the BGU model is given in Table 2.

$$\Delta\sigma = \Delta\sigma_y + \eta(\Delta\sigma_m - \Delta\sigma_y) \quad (5)$$

$$\Delta\sigma = \Delta\sigma_r + \eta(\Delta\sigma_m - \Delta\sigma_r) \quad (6)$$

Table 2 $\eta - \lambda$ input for the BGU model [6]

Pair	1	2	3	4	5	6	7	8
λ	0	2.80E-05	5.00E-05	9.00E-05	1.70E-04	3.00E-04	5.50E-04	1.00E-03
η	0	0.700	0.900	1.000	0.900	0.750	0.540	0.330
Pair	9	10	11	12	13			
λ	1.65E-03	2.50E-03	3.50E-03	7.00E-03	1.00E+10			
η	0.170	0.090	0.032	0.005	0			

Similar to reinforcement, the strain rate effect is recognised through the DIF applied to the failure surface of concrete as well. The CEB-FIP model code 1990 [7] introduces a set of formulas to calculate the DIFs. Malvar and Ross [8] agreed with the CEB-FIP model in compression (Eq.7) and modified the model in tension (Eq.8). In the latest fib model code 2010 [9], the formulas are slightly changed to simplify the calculation process. As for the concrete utilised for the Tsinghua test

specimen, the DIFs resulted from the abovementioned three methods are calculated and compared in Fig.2. It can be observed that the latest fib model tends to be more conservative than others when the strain rate effect is considered. In this study, Malvar and Ross' model is chosen as input and attached to the material keyword *MAT_CONCRETE_DAMAGE_REL3.

The CEB-FIP model for compressive strength:

$$\left.\begin{aligned} &\mathrm{DIF} = \left(\dot{\varepsilon}_c / \dot{\varepsilon}_{c0}\right)^{1.026\alpha_s} && \text{for } |\dot{\varepsilon}_c| \le 30\,\mathrm{s}^{-1} \\ &\mathrm{DIF} = \gamma_s \left(\dot{\varepsilon}_c / \dot{\varepsilon}_{c0}\right)^{1/3} && \text{for } |\dot{\varepsilon}_c| > 30\,\mathrm{s}^{-1} \end{aligned}\right\} \tag{7}$$

The modified CEB-FIP model for tensile strength:

$$\left.\begin{aligned} &\mathrm{DIF} = \left(\dot{\varepsilon} / \dot{\varepsilon}_s\right)^{\delta} && \text{for } \dot{\varepsilon} \le 1\,\mathrm{s}^{-1} \\ &\mathrm{DIF} = \beta\left(\dot{\varepsilon} / \dot{\varepsilon}_s\right)^{1/3} && \text{for } \dot{\varepsilon} > 1\,\mathrm{s}^{-1} \end{aligned}\right\} \tag{8}$$

in which, $\dot{\varepsilon}_c$ and $\dot{\varepsilon}$ are strain rates in compression and tension; $\dot{\varepsilon}_{c0} = -30\times10^{-6}\,\mathrm{s}^{-1}$, $\varepsilon_s = 10^{-6}\,\mathrm{s}^{-1}$; $\alpha_s = 1/(5+9f_c'/10)$, $\log\gamma_s = 6.156\alpha_s - 2$, $\delta = 1/(1+8f_c'/10)$ and $\log\beta = 6\delta - 2$.

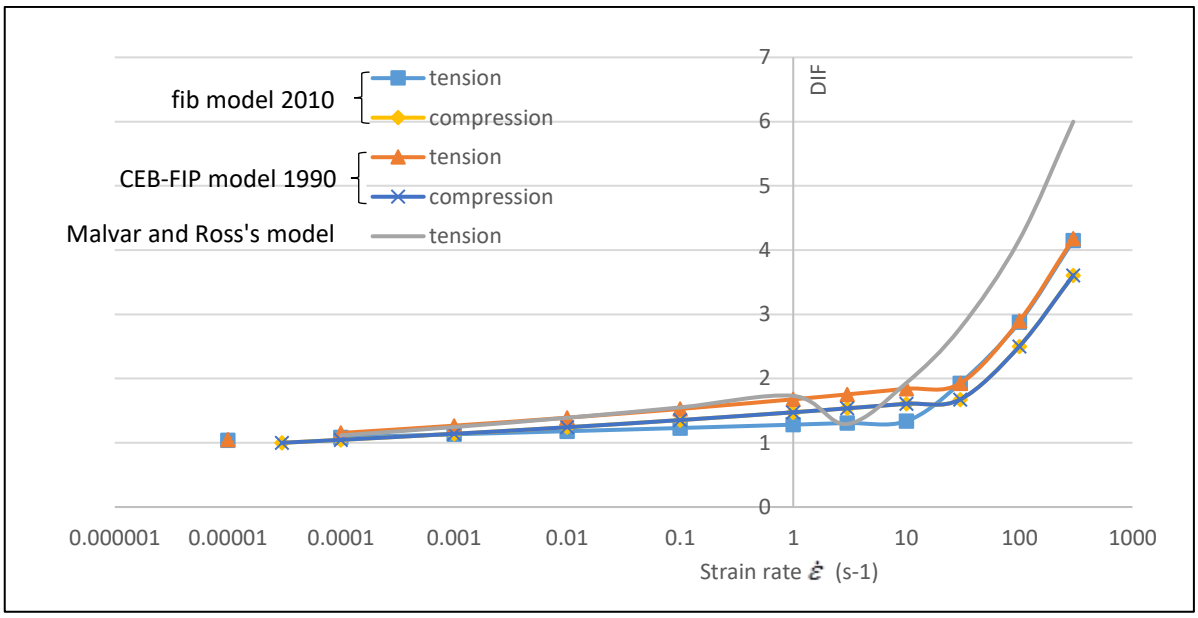

Fig. 2 DIF Comparison between three models

Other Settings. (1) Two layers of rigid body solid elements representing the hydraulic jack are added to the top surface of the column stub.

(2) In order to obtain the reaction force at the top of the column stub, which is equivalent to the applied load by the hydraulic jack, a cross section is defined through the keyword *DATABASE_CROSS_SECTION_SET. A set of nodes on the top surface of the column stub forms the cross section and a set of the top layer elements in the stub contributes to the internal force calculations.

Results and Discussion

Due to the complexity of input for the BGU model, the K&C model is firstly used to determine the force-displacement pattern and acquire a suitable loading history, with emphasise on the ultimate strength. Typical structural responses of the K&C model subject to three loading periods of 2s, 5s and 10s are shown in Fig.3. It can be seen that similar ultimate strengths are obtained for the loading periods 5s and 10s, whereas the ultimate strength is slightly larger for the 2s loading period. This implies that the loading history does not affect the ultimate strength when the loading period is greater than 2s, under which the inertial and damping actions can be neglected.

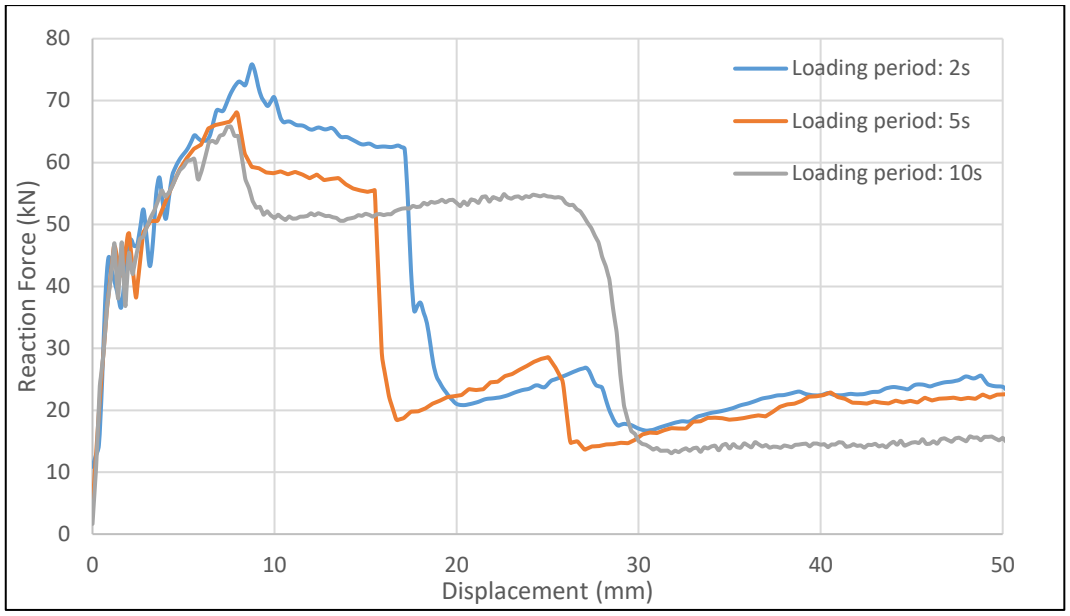

Fig. 3 Punching shear comparison between K&C models with different loading histories

Subsequently, the BGU model is applied to predict the force-displacement relationship which is also compared to the experimental result as shown in Fig. 4. Following observations can be made from the comparison. (1) The initial stiffness and the ultimate strength of the numerical model are in a good agreement with the experiment. (2) Numerically, there is an obvious sudden drop in the reaction force (at 50 mm) representing the punching shear failure, which manifest that the micro numerical model is capable of capturing such brittle failure phenomenon. However the predicted stage (or timing) of punching shear failure (at 50 mm) deviates from the experiment (at 41 mm). This is largely due to the relatively "fast" strengthening rate with respect to the effective plastic strain as compared to softening in the numerical analysis, which does not reflect the true concrete plastic behaviour in the experiment. Such a discrepancy also leads to a more flexible prediction after punching occurs. (3) Nevertheless, the strengthening behaviour post the punching shear failure is well simulated as the reaction force tends to rise again following the experimental trend. This is because the reinforcement can continue to carry the applied load after the capacity of concrete is completely lost within the critical perimeter of the column.

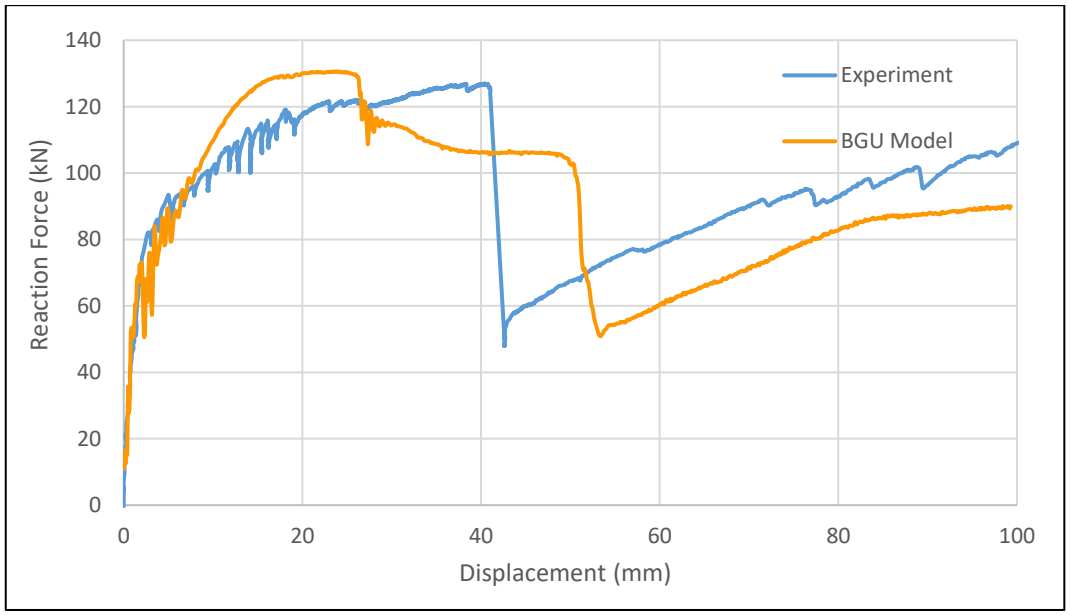

Fig. 4 Punching Shear Comparison between the BGU Model and the Experiment

Given that the predicted timing of the punching shear failure is different from the experimental one, further calibration of the numerical model is thus required. Improvements can be made by modifying the material properties as follows: (1) Adjust the strengthening and softening rate in terms of effective plastic strain to allow the model attain the ultimate strength with a larger plastic strain. (2) Use the keyword *MAT_ADD_EROSION with maximum shear strain criterion option to manage the timing of the punching shear failure. (3) The bonding and sliding between concrete and reinforcement elements are significant factors to reflect the membrane action after punching occurs. These factors should be taken into consideration in future work by using the keyword *CONTACT_1D.

The calibrated material properties are expected to be able to predict the experimental behaviour of all the specimens tested in the same batch. Subsequently, the same modelling procedures will be applied to calibrate the numerical model against other published experiments with different material strengths. Ultimately, this study will facilitate the development of an effective, yet simplified numerical model for future progressive collapse simulation of slab-column connections.

Conclusion

A numerical method for investigating post punching shear behaviour of a slab-column joint using a micro model is illustrated with emphasis on the material properties. Numerical results demonstrate that the model is capable of simulating the punching shear failure and post punching strengthening behaviour. A calibration approach is suggested based on the analysis of a typical structural response of the model, which will be exercised in the future work. It is expected that the proposed micro model will lay a foundation for the development of an effective, yet simplified numerical model for progressive collapse studies in the future.

Acknowledgements

This contribution is the result of the research supported by the Australian Research Council through an ARC Discovery Project (DP150100606).

References

[1] LS-DYNA Dev, LS-DYNA Theory Manual, Livermore Software Technology Corporation, 2015.

[2] J. Jiang, X, Lu, Finite Element Analysis of Concrete Structures 2nd Ed., Tsinghua University Press, Beijing, 2013.

[3] L. J. Malvar, Review of Static and Dynamic Properties of Steel Reinforcing Bars, ACI Materials Journal, 95(5), 1998.

[4] L. J. Malvar, J. E. Crawford, J. W. Wesevich, D. Simons, A Plasticity Concrete Material Model for DYNA3D, International Journal of Impact Engineering, 19(9-10), 1997.

[5] L. E. Schwer, L. J. Malvar, Simplified Concrete Modeling with *MAT_CONCRETE_DAMAGE_REL3, JRI LS-DYNA User Week, 2005.

[6] N. Markovich, E, Kochavi, G, Ben-Dor, An Improved Calibration of the Concrete Damage Model, Finite Elements in Analysis and Design, 47(2011).

[7] Comite Euro-International du Beton, CEB-FIP Model Code 1990, Thomas Telford, London, 1993.

[8] L. J. Malvar, C. A. Ross, Review of Strain Rate Effects for Concrete in Tension, ACI Materials Journal, 95(6), 1998.

[9] International Federation for Structural Concrete, fib Model Code for Concrete Structures 2010, Ernst & Sohn, Berlin, 2013.